Atmospheric Environment 316 (2024) 120180

Contents lists available at ScienceDirect

Atmospheric Environment

journal homepage: www.elsevier.com/locate/atmosenv

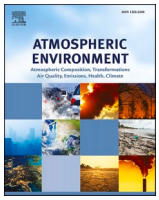

An assessment of natural and anthropogenic influences on atmospheric fluoride deposition in central Tibetan Plateau during 1951–2008 A.D. using the Zangser Kangri ice core

Xiang Zou [a,b], Wangbin Zhang [b], Shuangye Wu [c], Jinhai Yu [b], Jing Song [b], Hongxi Pang [b], Yaping Liu [d], Shugui Hou [b,e,*]

[a] School of Geography, Geomatics, and Planning, Jiangsu Normal University, Xuzhou, 221116, China
[b] School of Geography and Ocean Science, Nanjing University, Nanjing, 210023, China
[c] Department of Geology and Environmental Geosciences, University of Dayton, Dayton, OH, 45469, USA
[d] State Key Laboratory of Cryospheric Science, Northwest Institute of Eco-Environment and Resources, Chinese Academy of Science, Lanzhou, China
[e] School of Oceanography, Shanghai Jiao Tong University, Shanghai, 200240, China

HIGHLIGHTS

- A new annually resolved record of atmospheric fluoride deposition for the period 1951–2008.
- F^- concentrations derived from anthropogenic emissions were quantified using ice core record.
- Indian monsoon largely contributes the transport of anthropogenic fluoride.

ARTICLE INFO

Keywords:
Fluoride contamination
Tibetan Plateau
Ice core
Source analysis
Atmospheric transport

ABSTRACT

Fluoride contamination poses great threat to ecosystems and human health, and has caused widespread concern. Large gaps in knowledge still exist regarding the distribution, sources of fluoride and the influence of atmospheric transport on its dispersal, particularly at high altitudes because of a lack of data due to geographic constraints. Tibetan ice cores are a natural archive for chemical depositions from the atmosphere, and can be used to reconstruct past variations of atmospheric fluoride in remote environment. In this study, we investigate the trends, sources and controlling factor of atmospheric fluoride during 1951–2008 AD using high-resolution chemical deposition records derived from the Zangser Kangri (ZK) ice core, central Tibetan Plateau (TP). Our data shows that the concentration peaks of F^- coincide with those of typical crustal species (e.g., Ca^{2+}, Mg^{2+}), indicating that variation of F^- in the ZK ice core is largely driven by dust activities, and dust emission from soil is the primarily natural source of F^-. F^- sources and transport pathways were further investigated by using the empirical orthogonal function (EOF) analysis, excess (Ex) concentration, in combination with airmass backward trajectory analysis. Ex F^- in the ZK ice core record could be attributed to anthropogenic emissions, and its significant increase since 1990 was likely related to increased industrial and agricultural activities in the northwestern Indian peninsula. In addition, the strength of the South Asian monsoon is also a key factor in the transport of anthropogenic fluoride to the ZK glacier. This study provides valuable data for understanding the past atmospheric fluoride budget in the central TP.

1. Introduction

Fluorine is the 13th abundant element in the earth's crust, and the most common and lightest halogen with highest electronegativity in the natural environment (Fordyce et al., 2007; Jha et al., 2011). Fluoride contamination can lead to many problems for both ecosystems and human health (Mehta, 2013). Although trace amount of fluoride is beneficial to human growth, high fluoride intake can cause dental

* Corresponding author. School of Geography and Ocean Science, Nanjing University, Nanjing, 210023, China.
E-mail address: shuguihou@sjtu.edu.cn (S. Hou).

https://doi.org/10.1016/j.atmosenv.2023.120180
Received 25 May 2023; Received in revised form 27 October 2023; Accepted 31 October 2023
Available online 2 November 2023
1352-2310/© 2023 Elsevier Ltd. All rights reserved.

fluorosis, skeletal fluorosis and other diseases in humans (Kashyap et al., 2021). Fluorosis has become a prominent health concern in many countries around the world, especially in China and India, and received widespread attention from many disciplines (Srivastava and Flora, 2020). In addition, fluoride contamination has significant biological effects on vegetation. Fluoride can penetrate into plant tissue and affect plant metabolism, thereby altering the structure and composition of plant communities (Li et al., 2021). The distribution of fluoride has been extensively studied in industrialized and agricultural areas, but knowledge of the atmospheric fluoride deposition is lacking in remote high-altitude environment due to sampling and monitoring challenges. This limits the understanding of the global geochemical cycle of fluorine.

The Tibetan Plateau (TP), known as the "roof of the world", is the highest (over 4000 m on average) and most extensive highland (3.08 million square kilometers) in the world (Chen et al., 2022; Xu et al., 2014), with the most glaciers outside the polar regions (Yao et al., 2012). These glaciers receive and store atmospheric pollutants transported by westerlies and monsoons, which could be released back to the environment through increased snow melt under climate change (Zhao et al., 2013). Therefore, it is of great significance to understand the distribution and trend of fluoride concentrations in the glaciers, since the quality and safety of glacial meltwater in this region is related to the drinking water safety of billions of people downstream (Zhao et al., 2020). Ice core is a valuable tool to examine past climate and environmental change. Contiguous and high-resolution ice core records can provide important information of anthropogenic and natural emissions to the fluoride deposition (Preunkert et al., 2001; De Angelis and Legrand, 1994), as well as past atmospheric conditions and circulation patterns in remote areas.

Previous studies of Tibetan ice core have successfully reconstructed the variation of atmospheric chemical composition over the past century. They reveal that surrounding anthropogenic activities have profoundly affected the glacier chemical records. For instance, in the western TP, the records of Muztagata ice core show an increase in anthropogenic ammonium since the 1940s (Zhao et al., 2008), and a surge of anthropogenic sulfate and nitrate in the 1970s (Zhao et al., 2011). In the southern TP, the records of East Rongbuk ice core show that enhanced agricultural activities and energy consumption have contributed to the anthropogenic input of ammonium since the 1950s (Hou et al., 2003; Kang et al., 2002). In the central TP, anthropogenic inputs of sulfate and nitrate were observed in the second half of the 20th century based on nitrogen isotopes in the Qiangtang ice core (Li et al., 2020) and major ion concentrations in the Tanggula ice core (Zheng et al., 2010). The above glacier chemical records have greatly improved our understanding of the atmospheric chemical composition of the TP. They confirm that the Tibetan atmospheric environment has been significantly affected by anthropogenic activities from the surroundings regions since the 1950s. However, there are few data on the distribution, sources and trends of atmospheric fluoride deposition in TP during this period. The only assessment of the atmospheric fluoride budget over the past few decades has been conducted in the Laohugou ice core, the northeastern TP (Cui et al., 2010).

In this study, we present a high-resolution time series of F^- concentrations for the period 1951–2008 AD using the Zangser Kangri (ZK) ice core from central TP. This study aims to: (1) examine the temporal and spatial distribution of atmospheric F^- concentrations in central TP; (2) investigate the atmospheric fluoride sources and the impact of dynamic processes; (3) assess the contributions from anthropogenic and natural emissions. This study could enhance the understanding of fluorine geochemical cycles in remote areas.

2. Site description

The ZK glacier is located on the Qiangtang Plateau in central TP, surrounded by the mountains of Tanggula, Nyainqentanglha, and Gandisê Ranges (Fig. 1). This area is characterized by the typical arid and semi-arid continental climate, and is under the influence of the humid Indian monsoon in summer and the dry westerlies in winter (Yao et al., 2013). Previous studies, based on measured water vapor isotope data, found that the Indian monsoon can reach the ZK glacier at the central TP, implying its importance in transporting atmospheric chemicals to the ZK glacier (Tian et al., 2007). The records from the nearby meteorological stations show the local monthly mean temperature ranges from −10.8 °C in January to 10.7 °C in July, and the annual mean temperature is 0 °C. The annual mean precipitation is 257 mm, 75% of which falls between June and September (Zou et al., 2020b). The ZK glacier has an area of 337.98 km^2 and a volume of 41.70 km^3 with an average annual accumulation rate of 190 mm w.e. $year^{-1}$ (Shi et al., 2008; Zou et al., 2020b). Thus, the geographical conditions of this region are favorable for the preservation of glaciochemical records.

3. Methods

3.1. Sample collection

In April 2009, two ice cores to bedrock, Core 1 (127.7 m) and Core 2 (126.7 m), were retrieved from the ZK glacier (at 34°18′ N, 85°51′ E; 6226 m above sea level (a.s.l)) (Fig. 1) through a dry borehole with an electric drill. The borehole temperature varied from −15.2 °C to −9.2 °C, favorable for the preservation of the ice cores, as the samples were not affected by melting. Ice cores were placed in a freezer and transported to the State Key Laboratory of Cryospheric Science (SKLCS) in the city of Lanzhou. This study used the top 16.38 m of core 1. The core segments were cut in a cold room (~−20 °C) at a resolution of 4–6 cm with a stainless-steel band saw. The samples were then scraped with a ceramic knife in an ultra-clean laboratory (class 100) to remove the outer layer to prevent contamination. The operator changed disposable gloves and washed the ceramic knife with ultrapure water before processing each sample to minimize possible contamination. The shavings of ice core samples from the top 39.54 m were collected for β activity analysis.

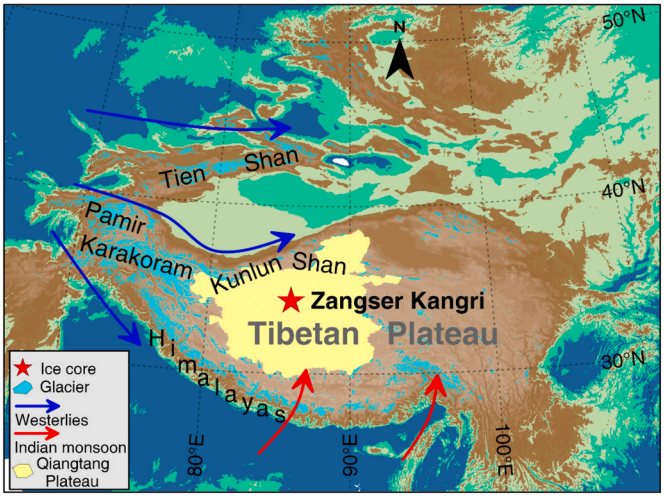

Fig. 1. Map of the Tibetan Plateau with the location of Zangser Kangri ice core drilling site (red star). This area is dominated by the Indian monsoon (red arrows) in summer and westerlies (blue arrows) in winter (Yao et al., 2012). The topographic data were extracted using ETOPO1 elevations global data, available from the National Oceanic and Atmospheric Administration (NOAA) at http://www.ngdc.noaa. gov/mgg/global/global.html (last access: August 20, 2023).

3.2. Chemical analysis and quality control

The chemical analyses included major soluble ions, water stable isotopes and β activity. The ice core samples were first thawed at room temperature (20 °C). They were then measured for the concentrations of major cations (Na^+, NH_4^+, K^+, Mg^{2+} and Ca^{2+}) and anions (Cl^-, SO_4^{2-}, NO_3^- and F^-) with the Dionex-600 and ICS-2500 ion chromatographs in the SKLCS laboratory. The cations were analyzed with a CS12 4 mm column, 200 μL loop column and isocratic 18 mM methanesulfonic acid (MSA) eluent; and the anions were analyzed with an AS11-HC 4 mm column, 500 μL loop column and isocratic 25 mM potassium hydroxide (KOH) eluent. For quality assurance and quality control (QA/QC), a standard solution (Chinese National Standards) and a laboratory blank (ultrapure water) were measured after every ten samples, and the results were used to calibrate the analytical procedure. A linear calibration curve was obtained by measurements of standard solutions diluted with ultrapure water (Milli-Q, 18.2 MΩ) and the correlation coefficients were greater than 0.999. The limit of detection (LOD), defined as the concentration measured by the analytical instrument at a signal-to-noise ratio × 3. The LOD for F^- is 0.3 ppb. All ultrapure water blank values are lower than the LOD. The relative standard deviation (RSD) for replicate was <5%. The precision of the method was determined by running 10 consecutive samples, which is less than 0.1%. Detailed information about the instrumentation for ion determination can be found in Tables S1 and S2 and Fig. S1. The samples were measured for water stable isotope composition with a Picarro L2120-i Cavity Ring-Down Spectrometer at the Ministry of Education Key Laboratory for Coast and Island Development, Nanjing University. β activity was measured at SKLCS with a MINI20 low background α/β counting system.

3.3. Ice core chronology

The ice core chronology was constructed with the annual layer counting method based on seasonal cycles of Ca^{2+}, SO_4^{2-} concentrations and $\delta^{18}O$ value. The Ca^{2+} concentration peaks are associated with winter/spring with high wind and dust load, whereas high $\delta^{18}O$ values indicate high temperatures in summer. In addition, the global peak of β activity in 1963 was used to constrain the chronology of ZK ice core. More details of dating methods and result could be found in Zou et al. (2020b) and Zhang et al. (2017).

3.4. Airmass trajectory analysis

To establish the sources of atmospheric fluoride deposition in the ZK ice core, we calculated the 7-day backward trajectories for air mass originated at the drilling site at 0:00, 6:00, 12:00 and 18:00 for every day for the period 1951–2008 AD using the Hybrid Single-Particle Lagrangian Integrated Trajectory (HYSPLIT) model. The HYSPLIT model was developed by the National Oceanic and Atmospheric Administration (NOAA) Air Resources Laboratory (ARL) and has been widely used to track wildfire smoke, windblown dust, air pollution and water vapor combined with moisture (Stein et al., 2015). It is also widely used to investigate sources of contaminants in ice cores (Grigholm et al., 2017; Wei et al., 2021; Zhang et al., 2017).

3.5. Statistical analysis

In this study, the empirical orthogonal function (EOF) analysis was conducted to identify the covariance characteristics, and trace common sources and transport pathways of multiple ions. EOF analysis allows robust assessment of relationships between multiple variables (Meeker et al., 1995). This method can avoid the influence of dating error on the multivariable relationship and is validated by chemical records in multiple ice cores (Wang et al., 2019; Zheng et al., 2010). In addition, to extract potential anthropogenic inputs of fluoride concentrations, excess (Ex) F^- concentrations were calculated using the following formula (Sierra-Hernández et al., 2018; Zou et al., 2020a):

$$Ex = X\text{-}[X/Na]_{\text{pre-industrial ice}} \times [Na]$$

where X represents the concentration of the target element (i.e. F^-) in this study, and $[X/Na]_{\text{pre-industrial ice}}$ represents the target element to Na ratio before the Industrial Revolution, which was established using the ice core records for the period 1800–1850 AD.

4. Results and discussion

4.1. The trends of F^- concentrations

The annual F^- concentrations from 1951 to 2008 were presented in Fig. 2a. The F^- concentrations of the ZK ice core during this time range from 0.86 ng g^{-1} to 10.48 ng g^{-1}, with a mean concentration of 3.90 ng g^{-1}, which is an order of magnitude higher than the mean F^- concentrations in Greenland ice cores (0.19 ng g^{-1}, 1971–1989) (De Angelis and Legrand, 1994). This suggests that atmospheric fluoride concentrations are closely related to proximity to emission sources. We further calculated the 5-year running average of F^- concentrations to remove short-term interannual variability in order to examine decadal trends and variabilities (Fig. 2a). Before 2000, the smoothed F^- concentrations show several peaks around 1968, 1978, 1986 and 1995, which coincided with peaks in Ca^{2+} (a proxy of dust) and other soluble ions (Fig. 3). This suggests that F^- concentrations before 2000 were largely driven by dust activities. After 2000, the F^- concentrations show a significant upward trend until the end of the record at 2008, with a mean concentration 1.49 times higher than the Pre-2000 mean. However, the increase in F^- concentration during this period did not correspond to the trend in dust activities, and was therefore likely caused by an increase in anthropogenic input for the period. This increase in anthropogenic input was supported by some previous studies. For example, Sierra-Hernández et al. (2019) reported a significant increase in the excess concentrations and enrichment factors of heavy metals from the nearby Guliya ice core (Cd, Zn, Pb, and Ni) during the 2000–2015 period relative to that of the 1971–1990 period. However, Fig. 3 shows no significant increase in

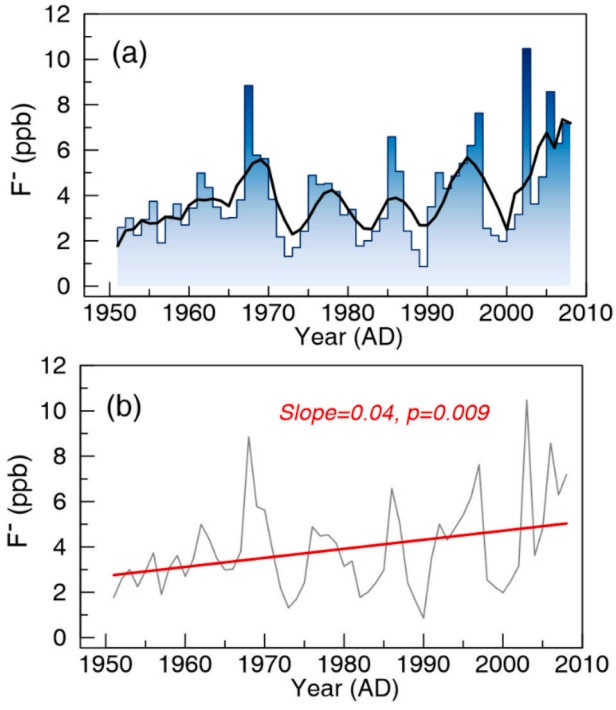

Fig. 2. (a) the annual F^- concentrations (ppb) for 1951–2008 AD, and 5-year running average (bold black line); (b) the linear trend of F^- for 1951–2008 AD.

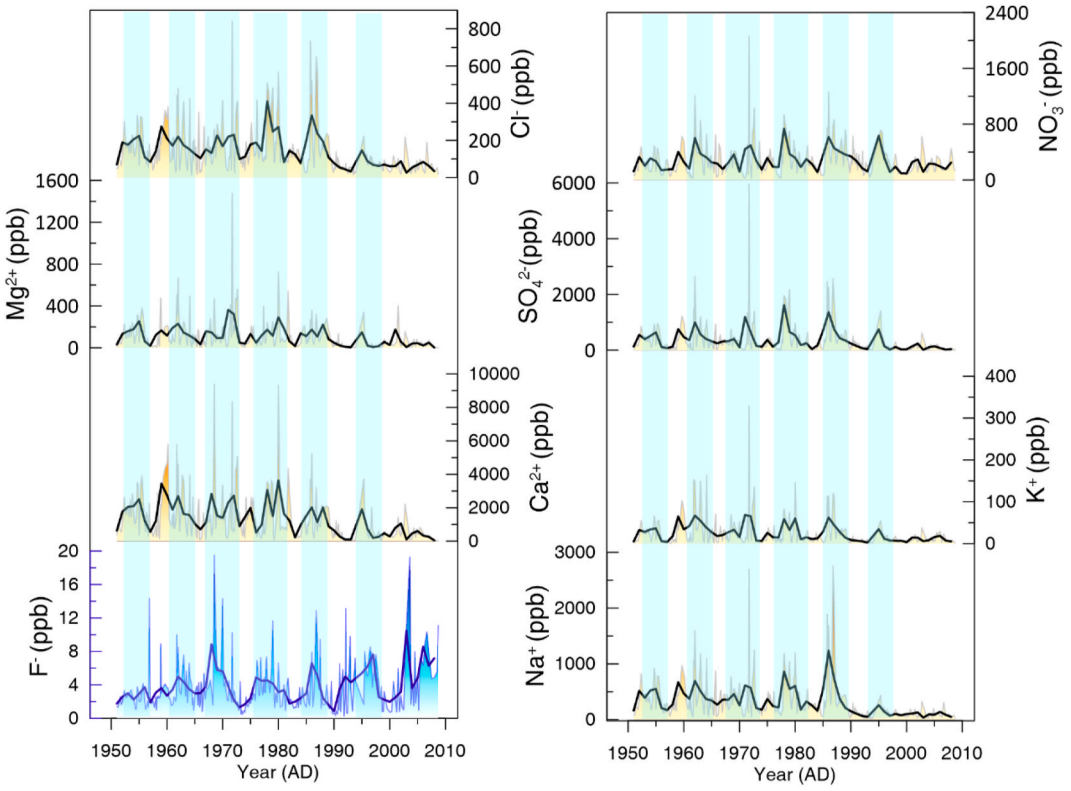

Fig. 3. The raw concentrations (grey lines) and annual concentrations (bold black lines) of Cl^-, Mg^{2+}, Ca^{2+}, F^-, NO_3^-, SO_4^{2-}, K^+ and Na^+. Blue shaded areas indicate period of common peaks in major ions concentrations.

sulfate and nitrate in the ZK ice core during this period, despite the opposite results found in some previous studies in the western Tibetan ice cores (Zhao et al., 2011). This discrepancy could be due to the difference in dust activities, which are more dominant in their control over the variability of ion concentration in the central than western Tibetan glaciers. As a result, it is more difficult to detect anthropogenic inputs in the raw concentration data in central Tibet. Similar results were found in the Qiangtang ice core, also located in central TP (Wang et al., 2019). In another study, using nitrogen isotope records from Qiangtang ice core, Li et al. (2020) found an increasing trend of anthropogenic nitrate input from South Asia since 1950, although NO_3^- showed no such increase. These studies further suggest that anthropogenic input in the central Tibetan glaciers could be masked by dust activities.

4.2. Source analysis

The EOF analysis is a commonly used method to study potential interspecies associations and the transport pathways of major soluble ions, and could help identify environmental conditions controlling the glaciochemistry of ZK ice core. We performed the EOF analysis on the annual mean concentrations of Ca^{2+}, Mg^{2+}, Na^+, K^+, Cl^-, NO_3^-, SO_4^{2-} and F^-, and the results are presented in Table 1. The first three EOFs together explain ~91.40 % of the total variance. EOF 1 explains 70.79 % of the variance, with strong loadings from all ions except F^-. This strong interspecies relationships in the ZK ice core were further confirmed by high correlations among major soluble ions (Table 2). The high loadings of crustal elements such as Ca^{2+} and Ma^{2+} (proxies for dust) on EOF 1 indicate that the variations in the ZK ice core chemical records were primarily driven by dust activities. EOF 2 accounts for 13.35% of the total variance and is highly loaded by F^- (0.96), and partial loaded by NO_3^- (0.12), SO_4^{2-} (0.18). The EOF 2 series (Fig. 4) represents sources independent of dust and coincides with Ex F^- concentrations. Therefore, EOF 2 likely reflects the inputs from anthropogenic emission activities. EOF 3 is dominated by Ca^{2+} and Mg^{2+}, and represents 7.26 % of the total variance. This likely represents a secondary emission of local crustal dust, which was also present in other glaciochemical records in the central TP (Wang et al., 2019).

In order to investigate the sources of atmospheric pollution for the

Table 1
The statistical summary of EOF analysis of annual ions concentrations in the ZK ice core.

	EOF 1	EOF 2	EOF 3	Communality
Na^+	0.94	0.06	−0.10	0.98
K^+	0.95	0.07	0.11	0.94
Mg^{2+}	0.82	−0.24	0.41	0.98
Ca^{2+}	0.88	−0.16	0.31	0.99
Cl^-	0.93	0.00	−0.05	0.97
F^-	−0.04	0.97	0.26	1.00
SO_4^{2-}	0.94	0.12	−0.22	0.96
NO_3^-	0.82	0.18	−0.43	0.99
Variance (%)	70.79	13.35	7.26	
Cum.Variance (%)	70.79	84.14	91.40	

Table 2
Correlation matrix of major soluble ion (raw data) in the ZK ice core for the period 1951–2008 AD, calculated from 296 samples. All correlations are significant at the 99 % confidence level.

	Na^+	K^+	Mg^{2+}	Ca^{2+}	F^-	Cl^-	SO_4^{2-}	NO_3^-
Na^+								
K^+	0.89							
Mg^{2+}	0.71	0.84						
Ca^{2+}	0.72	0.78	0.82					
F^-	0.33	0.35	0.26	0.30				
Cl^-	0.94	0.86	0.71	0.78	0.34			
SO_4^{2-}	0.90	0.89	0.76	0.70	0.31	0.85		
NO_3^-	0.79	0.82	0.64	0.63	0.28	0.75	0.87	

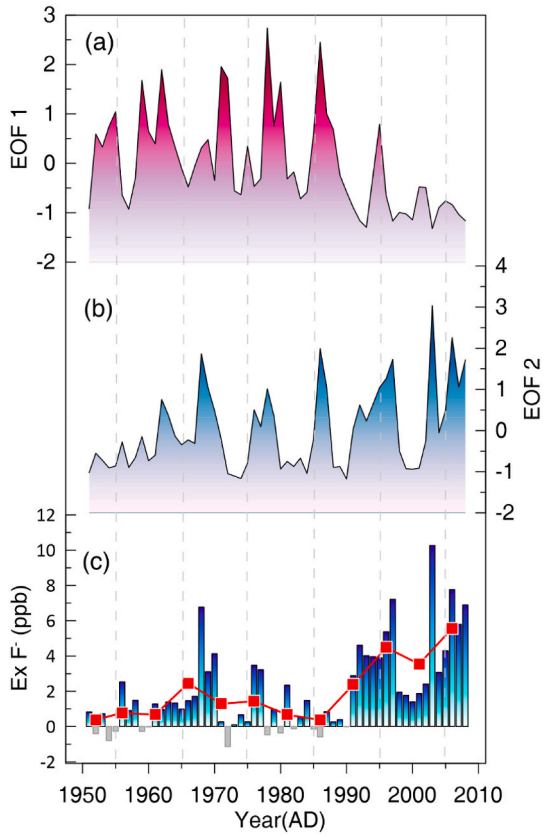

Fig. 4. (a) EOF 1 and (b) EOF 2 series calculated by EOF analysis for the period 1951–2008 AD. EOF 1 is primarily loaded by Na^+, K^+, Mg^{2+}, Ca^{2+}, Cl^-, SO_4^{2-}, NO_3^-. EOF 2 is separately loaded by F^-. (c) Excess F^- concentrations and 5-year mean concentrations (red line).

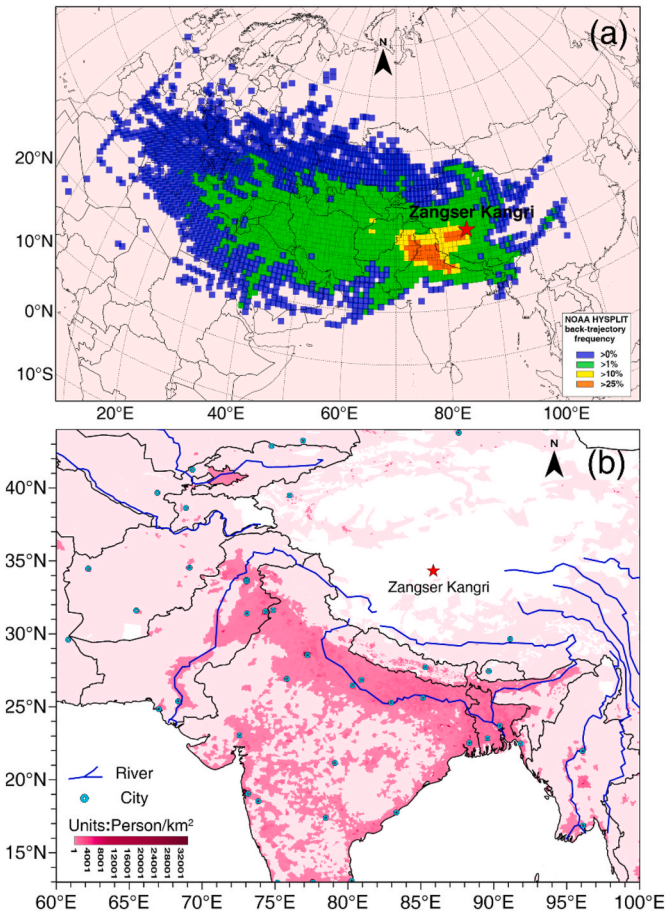

Fig. 5. (a) Normalized frequency plot of 7-day backward trajectories for the period of 1951–2008 AD calculated by NOAA HYSPLIT; (b) population density for 2000, from Center for International Earth Science Information Network (CIESIN, 2000). Population density data have 30 arc-second resolutions from the Gridded Population of the World (GPW) version v4, produced by CIESIN for the year 2000 and it is available at https://sedac.Ciesin.columbia.edu/data/collection/gpw-v4.

ZK glacier, we ran the HYSPLIT model to calculate the 7-day backward trajectory of the air mass from 1951 to 2008. Fig. 5a shows the normalized frequency of all trajectories. The results show that the highest frequencies (>25%) of backward trajectories were found in the Qiangtang Plateau and the northwestern Indian peninsula, including northern Pakistan and Indus-Ganges River Basin. This region has experienced intense industrial and agricultural activities since 1950, thus is likely to be the most important source of pollutants for the ZK glaciers. F^- from these regions is likely to be transported to the ZK glacier during the summer through the South Asian Monsoon. The expanded area of influence (i.e. frequency>5%) comprised of Central Asia, the Middle East, and northern Arabian Peninsula (Fig. 5a), although they make smaller contributions. F^- from these regions is mostly transported to the ZK glacier during the winter by the strong westerlies (Zou et al., 2022).

4.3. Contribution assessment

4.3.1. Natural sources

In this section, we investigate the impact of natural emissions on atmospheric fluoride budget in central TP. The major natural sources of atmospheric fluoride include volcanic eruptions, soil dust particles and sea-salt spray. A previous study of Greenland ice core suggested that the occasional fluoride peaks in the record were likely attributed to volcanic eruptions in Iceland and the Aleutian Islands (De Angelis and Legrand, 1994). However, due to short atmospheric lifetime of volcanic HF, the contribution of volcanic emissions to fluoride deposition decreases sharply with distance from the emission source (Fuge, 2019). This is the reason why the constant eruptions of Mount Etna (Sicily) contributed little to the fluoride records in the ice cores from the Alps (Preunkert et al., 2001). Paleoenvironmental reconstructions based on trace element Bi (a proxy for volcanic eruptions) in glaciers since the 1950s (Xu et al., 2009) found significant impacts from major volcanic eruptions in 1951 (Krut), 1963 (Agung) and 1991 (Pinatubo) on the atmospheric environment of the TP. However, we found no corresponding peaks of fluoride concentrations in the ZK ice core record, implying limited contributions from volcanic emissions. It is also likely that volcanic input may be overwhelmed by strong dust events and not easily detected in in TP glaciers.

A recent systematic survey of fluoride concentrations in surface waters of rivers and lakes on TP indicates that atmospheric F^- deposition is an important source to fluoride in remote areas (Yang et al., 2022). As early as the 1970s, Weinstein (1977) found that weathered soil particles contributed to the increase in atmospheric F^- concentrations. Moreover, studies of ice core from Greenland (De Angelis and Legrand, 1994) and the Alps (Preunkert et al., 2001) confirmed that soil-derived dust particles play an important role for the atmospheric F^- deposition in precipitation. In the natural environment, fluoride-bearing minerals like fluorite (CaF_2), fluorapatite ($Ca_5(PO_4)_3F$), sallaite (MgF_2), villiaumite (NF), apatite, etc., and certain clays are important sources of aeolian particles of atmospheric fluoride (Schlesinger et al., 2020). Given the abundant weathered dust on the surface of TP, the emission of fluorine-containing minerals could be an important natural source of F^- in the ZK ice core. Similar findings were also reported for the Laohugou ice core in the northeast of TP (Cui et al., 2010).

Apart from the natural emissions discussed above, marine-derived F^-

is also an important factor affecting its geochemical cycles (Schlesinger et al., 2020). However, marine-derived aerosols are unlikely to contribute to fluoride deposition in the ZK ice core due to its remote location. To confirm this, we calculated the fluoride fraction from non-sea salt sources using the following formula (Cui et al., 2010; Zhang et al., 2012):

$$SSx = R \times M$$

where SS_x represents sea salt source contribution of the target element; X represents the concentration of the target element; M is the sea-salt tracer ion concentration, and R is the ratio X/M of standard seawater (Nabipour and Dobaradaran, 2013). Cl^- was selected as the sea salt tracer ion, based on the Na^+/Cl^- and Mg^{2+}/Cl^- ratios that are greater than those of standard sea-water ($Na^+/Cl^- = 0.86$, $Mg^{2+}/Cl^- = 0.20$). The result shows that the sea-salt contribution accounted for less than 1% of F^- in the ZK ice core. The contribution of sea-salt aerosols to the chemical composition of the atmosphere decreases with increasing distance from the coast, and it is difficult for fluorinated aerosols from the Indian Ocean to reach the hinterland of the TP (Klopper et al., 2020; Okita et al., 1974; Torres-Sánchez et al., 2019).

4.3.2. Anthropogenic sources

Since the Industrial Revolution, increased anthropogenic emissions have significantly affected the Earth system by altering the geochemical cycles of element (Sen and Peucker-Ehrenbrink, 2012; Kamenov et al., 2009). The chemical records from the Tibetan ice cores also revealed strong influence on the atmospheric depositions from surrounding anthropogenic inputs since the 1950s (Hou et al., 2003; Zhao et al., 2008; Zheng et al., 2010). To investigate potential anthropogenic sources of atmospheric F^-, Ex F^- concentrations were calculated (see Section 3.5) and presented in Fig. 4c. The record shows two periods of high Ex F^- concentrations: 1960–1970 AD and 1990–2008 AD. Moreover, it also shows a significant increase in Ex F^- since 1990 based on the 5-year mean concentration trend (Fig. 4c), suggesting intensified anthropogenic input during this period.

Anthropogenic input of atmospheric F^- in central TP primarily comes from both industrial emissions (such as coal combustion, brickmaking, aluminum smelting), and agricultural emissions (such as application of phosphate fertilizer and the practice of stubble burning) (Fuge, 2019). Due to the extensive fluorine content in clay minerals and mica used for brick making, up to 85.4% of fluorides (mainly HF and SiF_4) are released to the environment during the production process in a high temperature environment (1100 °C) (Weinstein and Davison, 2004; Xie et al., 2003). India is the second largest brick-making country in the world, with brick factories in the suburbs of all major cities (Kumbhar et al., 2014). These factories emit a large amount of fluoride into the environment due to poor management (Ahmad et al., 2012). The global average fluorine concentration in coal is as high as 88 mg kg^{-1}, and at a high temperature of 800 °C, 80% of the fluorine in coal is released into the environment in gaseous and particulate forms (Fuge, 2019; Ketris and Yudovich, 2009). Therefore, coal combustion is the primarily source of industrial emission with estimated annual fluorine flux of 12,000–102,000 t (Jayarathne et al., 2014; Tavener and Clark, 2006). Similarly, in the process of aluminum smelting, cryolite (Na_3AlF_6), as a co-solvent for electrolysis aluminum production, can release fluoride into the environment at high temperatures of 960 °C (Fuge, 2019). In agriculture, the application of phosphate fertilizer is a non-negligible anthropogenic source of atmospheric fluoride (Schlesinger et al., 2020). According to Ramteke et al. (2018), commonly used phosphate fertilizers (Single superphosphate, Diammonium phosphate, Ammonium nitrophosphate) in India contain 3.14–74.8% original F^- (Ramteke et al., 2018). In soils fertilized by phosphates, high concentrations of fluoride accumulate in this area as fluoride are typically adsorbed by clay minerals, aluminum oxyhydroxides, and iron oxyhydroxides, which eventually become a potential source of atmospheric fluoride (Fuge, 2019).

As important potential source regions for atmospheric pollutants arriving in the ZK ice core site, Pakistan and India have experienced a significant population increase trend from 1951 to 2008 (Fig. 6). Population density is the highest along the Ganges and Indus rivers in the northern part of the Indian peninsula (Fig. 5b). The consequent increases in industrial and agricultural activities in this region could be major contributors to atmospheric fluoride in the ZK ice core record. Fig. 6 shows the historical trends of selected variables indicating such industrial and agricultural activities that might lead to F^- emissions. They all show significant increases since 1961, which is consistent with the 5-year mean Ex F^- concentration trend in ZK ice core. Therefore, the increase in atmospheric F^- content in the central TP region is likely to be attributed to anthropogenic activities in the northwestern part of the Indian peninsula.

4.4. South Asia monsoon influence

The South Asian summer monsoon plays an important role in transporting pollutants from anthropogenic activities in South Asia to the TP glaciers. This is confirmed by numerous studies in glacier chemical records and field monitoring data (Li et al., 2007; Zou et al., 2020b). In order to study the effect of South Asian monsoon activity on the trend of anthropogenic F^- concentration in the ZK ice core, we examined the correlation between the reconstructed South Asian summer monsoon index (SASMI) (Li and Zeng, 2002) and the Ex F^- concentration (Fig. 7). SASMI is a monsoon index developed by Li and Zeng (2002), and can be used to quantify the strength of Indian summer

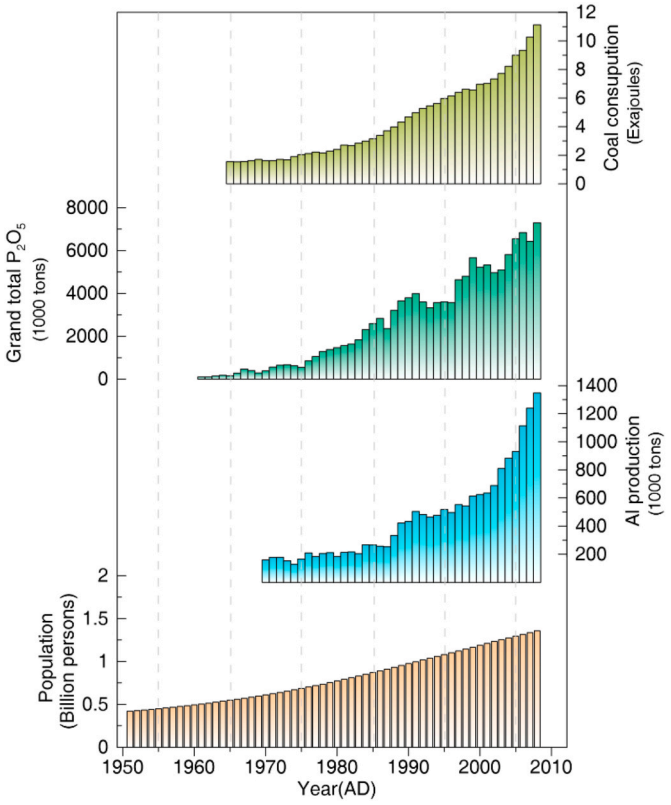

Fig. 6. Trends of coal consumptions for India and Pakistan (data from https://www.bp.com/en/global/corporate/energy-economics/statistical-review-of-world-energy/downloads.html), total P_2O_5 for South Asia (data from https://www.ifastat.org), aluminum (Al) production for India (data from https://www2.bgs.ac.uk/mineralsuk/statistics/worldArchive.html), population for India and Pakistan (data from https://www.fao.org/faostat/en/#data/OA). These are associated with industrial and agricultural activities contributing to fluoride emission for the period 1951–2008 AD.

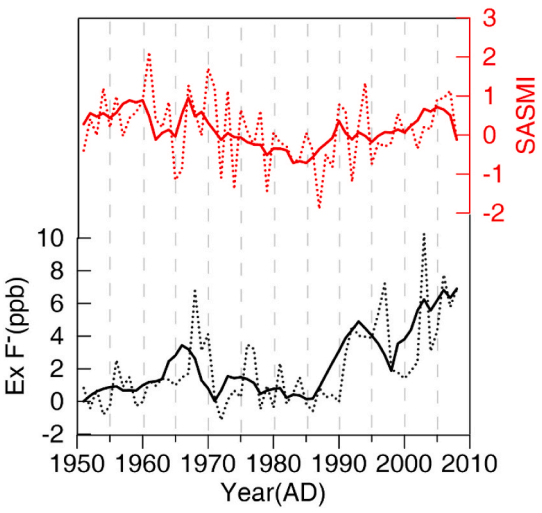

Fig. 7. Comparison of excess F^- concentration in the ZK ice core with the South Asian summer monsoon index (SASMI) during the period 1951–2008 AD.

monsoon. During the strong SASMI periods, greater land-sea thermal contrast leads to strong southwesterly winds during summer, which, in turn, transports more fluoride from the Indian Peninsula to the central TP. Our results show that two peaks (around 1968 and 1995, respectively) in the Ex F^- concentrations coincided with SASMI peaks, and that the increasing trend of the Ex F^- concentrations after the 1990s is consistent with a strengthening trend of SASMI (Fig. 7). In 2005, a decline in Ex F^- concentrations corresponded to a shift in the SASMI trend. This relationship was further confirmed by a statistically significant positive correlation ($r = 0.28$, $p < 0.05$) between the five-year running average concentrations of Ex F^- and SASMI. We performed the cross wavelet transform (XWT) and wavelet coherence (WTC) analysis between SASMI and annual F^- concentration for 1951–2008 AD (Fig. 8) (Grinsted et al., 2004). The XWT results show that the common high energy region occurred at a time scale of 7–10 years for 1961–1974 and 4–6 years for 1984–1994 (Fig. 8a). The WTC results show that significantly high wavelet coherence was found at a time scale of 2–3 years in 1965–1978 and 0–2 years in 1988–1996 (Fig. 8b). These significant resonance periods suggest that SASM has a significant effect on F^- deposition in ZK ice core during the above periods. These results suggest that the South Asian monsoon plays an important role in transporting fluorine-containing aerosols originated from South Asian anthropogenic emissions. Previous studies found that the Indian monsoon can reach the northern edge of the TP (~35°N) during the monsoon period (June–September), passing the study site (Zou et al., 2022). The present prevailing updraft below 200 hpa on the southern margin of the TP is favorable for transporting aerosols from the Indo-Gangetic Basin to the interior of the TP (Xu et al., 2014).

5. Conclusion

This study provided a detailed assessment of atmospheric fluoride deposition in central TP for the period 1951–2008, using the ZK ice core record. The mean F^- concentration in this area is an order of magnitude higher than that of the Greenland ice core during the same period, and the emission of F-bearing minerals after weathering is the main source of its natural activities. Linear regression analysis shows that the F^- concentrations have shown a slight upward trend since 1951. Coincided peaks of F^- and Ca^{2+} (a proxy for dust) indicate that its primarily natural source is soil particle deposition driven by wind activity. Based on empirical orthogonal function (EOF) and Ex concentration analysis, F^- concentrations contributed from anthropogenic emissions were quantified and showed a significant upward trend since 1990. And analysis of backward trajectories of airmass shows that the pollutants in the ZK glacier mainly come from the northwestern part of the Indian peninsula. Based on a survey of potential anthropogenic emissions of atmospheric F^- in this region, the significantly increased anthropogenic emissions since 1961 likely contributed to the enrichment of F^- in the ZK ice core. In addition, the similar trends between SASMI and Ex F^- concentrations indicate that the South Asian monsoon plays an important role in transporting F-containing aerosols from anthropogenic emissions in South Asia. This study provides valuable insights into the biogeochemical cycles of fluorine in remote areas, filling the gaps in knowledge due to a lack of observation data.

CRediT authorship contribution statement

Xiang Zou: Data curation, Writing – original draft, Formal analysis. **Wangbin Zhang:** Software, Investigation. **Shuangye Wu:** Writing – review & editing. **Jinhai Yu:** Validation, Software. **Jing Song:** Software, Investigation. **Hongxi Pang:** Funding acquisition, Supervision. **Yaping Liu:** Investigation. **Shugui Hou:** Conceptualization, Funding acquisition, Methodology, Project administration, Supervision.

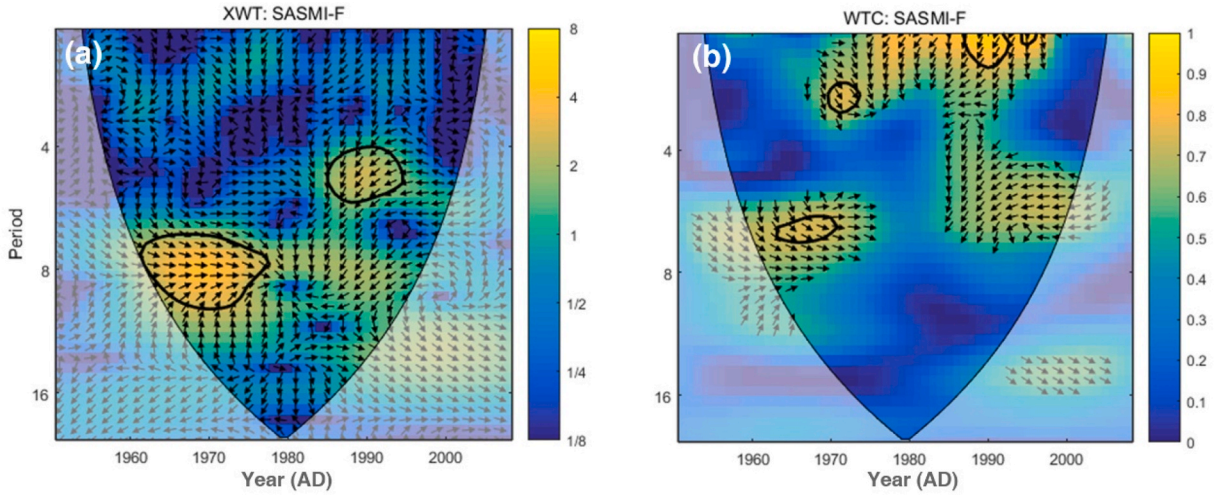

Fig. 8. Cross wavelet spectrum (a) and wavelet coherence spectrum (b) between SASMI and annual F^- concentration. Thick contours enclose regions of 5 % pointwise significance. Light shading corresponds to the cone of influence, the region in which edge effects become important. The relative phase relationship is shown as arrows (with in-phase pointing right, anti-phase pointing left, and the angle indicating time lags of two series).

Declaration of competing interest

The authors declare that they have no known competing financial interests or personal relationships that could have appeared to influence the work reported in this paper.

Data availability

The authors do not have permission to share data.

Acknowledgements

This work was funded by National Natural Science Foundation of China (41830644, 4202100, 42301137 and 42001050), the "333 Project" of the Jiangsu Province (BRA2020030), and the Natural Science Foundation of the Jiangsu Higher Education Institutions of China (No. 23KJB170007). We thank all the scientists, technicians, graduate students, and porters in the Zangser Kangri ice cap during the 2009 field work. The authors are grateful for the NOAA Air Resource Laboratory (ARL) for providing the HYSPLIT transport and dispersion model and READY website (http://www.ready.noaa.gov) used in this publication.

Appendix A. Supplementary data

Supplementary data to this article can be found online at https://doi.org/10.1016/j.atmosenv.2023.120180.

References

Ahmad, M.N., van den Berg, L.J., Shah, H.U., Masood, T., Büker, P., Emberson, L., Ashmore, M., 2012. Hydrogen fluoride damage to vegetation from peri-urban brick kilns in Asia: a growing but unrecognised problem? Environ. Pollut. 162, 319–324.
Center for International Earth Science Information Network, Columbia University, United Nations Food and Agriculture Programme, and Centro Internacional de Agricultura Tropical, 2000. Gridded population of the world, version 3 (GPWv3): population count grid. In: Palisades. NASA Socioeconomic Data and Applications Center (SEDAC). NY. (Accessed 19 August 2022).
Chen, F., Xia, H., Jia, Z., Zhang, D., 2022. Earliest hand-and footprint art indicates that Denisovans may have occupied the interior of the high-altitude Tibetan Plateau since 200 thousand years ago. Sci. China Earth Sci. 65, 769–772.
Cui, X.Q., Ren, J.W., Qin, X., 2010. Source of major ions from an ice core of the No. 12 glacier in Laohugou valley, qilian mountain. Science in Cold and Arid Regions 2 (6), 522–528.
De Angelis, M., Legrand, M., 1994. Origins and variations of fluoride in Greenland precipitation. J. Geophys. Res. Atmos. 99 (D1), 1157–1172.
Fordyce, F.M., Vrana, K., Zhovinsky, E., Povoroznuk, V., Toth, G., Hope, B.C., Iljinsky, U., Baker, J., 2007. A health risk assessment for fluoride in Central Europe. Environ. Geochem. Health 29 (2), 83–102.
Fuge, R., 2019. Fluorine in the environment, a review of its sources and geochemistry. Appl. Geochem. 100, 393–406.
Grigholm, B., Mayewski, P.A., Aizen, V., Kreutz, K., Aizen, E., Kang, S., Maasch, K.A., Sneed, S.B., 2017. A twentieth century major soluble ion record of dust and anthropogenic pollutants from Inilchek Glacier, Tien Shan. J. Geophys. Res. Atmos. 122 (3), 1884–1900.
Grinsted, A., Moore, J.C., Jevrejeva, S., 2004. Application of the cross wavelet transform and wavelet coherence to geophysical time series. Nonlinear Process Geophys. 11 (5/6), 561–566.
Hou, S., Qin, D., Zhang, D., Kang, S., Mayewski, P.A., Wake, C., 2003. A 154 a highresolution ammonium record from the Rongbuk Glacier, north slope of Mt. Qomolangma(Everest), Tibet-Himal region. Atmos. Environ. 37, 721–729.
Jayarathne, T., Stockwell, C.E., Yokelson, R.J., Nakao, S., Stone, E.A., 2014. Emissions of fine particle fluoride from biomass burning. Environ. Sci. Technol. 48 (21), 12636–12644.
Jha, S.K., Mishra, V.K., Sharma, D.K., Damodaran, T., 2011. Fluoride in the environment and its metabolism in humans. Rev. Environ. Contam. Toxicol. 211, 121–142.
Kamenov, G.D., Brenner, M., Tucker, J.L., 2009. Anthropogenic versus natural control on trace element and Sr–Nd–Pb isotope stratigraphy in peat sediments of southeast Florida (USA),~ 1500 AD to present. Geochem. Cosmochim. Acta 73 (12), 3549–3567.
Kang, S., Mayewski, P.A., Qin, D., Yan, Y., Zhang, D., Hou, S., Ren, J., 2002. Twentieth century increase of atmospheric ammonia recorded in Mount Everest ice core. J. Geophys. Res. Atmos. 107 (D21). ACL-13.
Kashyap, S.J., Sankannavar, R., Madhu, G.M., 2021. Fluoride sources, toxicity and fluorosis management techniques–A brief review. Journal of Hazardous Materials Letters 2, 100033.
Ketris, M.Á., Yudovich, Y.E., 2009. Estimations of Clarkes for Carbonaceous biolithes: world averages for trace element contents in black shales and coals. Int. J. Coal Geol. 78 (2), 135–148.
Klopper, D., Formenti, P., Namwoonde, A., Cazaunau, M., Chevaillier, S., Feron, A., Gaimoz, C., Hease, P., Lahmidi, F., Mirande-Bret, C., Triquet, S., Zeng, Z., Piketh, S. J., 2020. Chemical composition and source apportionment of atmospheric aerosols on the Namibian coast. Atmos. Chem. Phys. 20 (24), 15811–15833.
Kumbhar, S., Kulkarni, N., Rao, A.B., Rao, B., 2014. Environmental life cycle assessment of traditional bricks in western Maharashtra, India. Energy Proc. 54, 260–269.
Li, A., Wang, Y., He, Y., Liu, B., Iqbal, M., Mehmood, K., Jamil, T., Chang, Y., Hu, L., Li, Y., Guo, J., Pan, J., Tang, Z., Zhang, H., 2021. Environmental fluoride exposure disrupts the intestinal structure and gut microbial composition in ducks. Chemosphere 277, 130222.
Li, C., Kang, S., Zhang, Q., Kaspari, S., 2007. Major ionic composition of precipitation in the Nam Co region, Central Tibetan Plateau. Atmos. Res. 85 (3–4), 351–360.
Li, J., Zeng, Q., 2002. A unified monsoon index. Geophys. Res. Lett. 29, 115.
Li, Z., Hastings, M.G., Walters, W.W., Tian, L., Fang, Y., 2020. Isotopic evidence that recent agriculture overprints climate variability in nitrogen deposition to the Tibetan Plateau. Environ. Int. 138, 105614.
Meeker, L.D., Mayewski, P.A., Bloomfield, P., 1995. A new approach to glaciochemical time series analysis. In: Ice Core Studies of Global Biogeochemical Cycles, vol. 1995. Springer, Berlin, Heidelberg, pp. 383–400.
Mehta, A., 2013. Biomarkers of fluoride exposure in human body. Indian J. Dent. 4 (4), 207–210.
Nabipour, I., Dobaradaran, S., 2013. Fluoride and chloride levels in the Bushehr coastal seawater of the Persian Gulf. Fluoride 46 (4), 204–207.
Okita, T., Kaneda, K., Yanaka, T., Sugai, R., 1974. Determination of gaseous and particulate chloride and fluoride in the atmosphere. Atmos. Environ. 8 (9), 927–936.
Preunkert, S., Legrand, M., Wagenbach, D., 2001. Causes of enhanced fluoride levels in Alpine ice cores over the last 75 years: implications for the atmospheric fluoride budget. J. Geophys. Res. Atmos. 106 (D12), 12619–12632.
Ramteke, L.P., Sahayam, A.C., Ghosh, A., Rambabu, U., Reddy, M.R.P., Popat, K.M., Rebary, B., Kubavat, D., Marathe, K.V., Ghosh, P.K., 2018. Study of fluoride content in some commercial phosphate fertilizers. J. Fluor. Chem. 210, 149–155.
Schlesinger, W.H., Klein, E.M., Vengosh, A., 2020. Global biogeochemical cycle of fluorine. Global Biogeochem. Cycles 34 (12), e2020GB006722.
Sen, I.S., Peucker-Ehrenbrink, B., 2012. Anthropogenic disturbance of element cycles at the Earth's surface. Environ. Sci. Technol. 46 (16), 8601–8609.
Shi, Y., Li, S., Ye, B., Liu, C., Wang, Z., 2008. Concise Glacier Inventory of China. Shanghai Popular Science Press, Shanghai, China [in Chinese].
Sierra-Hernández, M.R., Beaudon, E., Gabrielli, P., Thompson, L., 2019wu. 21st-century Asian air pollution impacts glacier in northwestern Tibet. wu Atmos. Chem. Phys. 19 (24), 15533–15544.
Sierra-Hernández, M.R., Gabrielli, P., Beaudon, E., Wegner, A., Thompson, L.G., 2018. Atmospheric depositions of natural and anthropogenic trace elements on the Guliya ice cap (northwestern Tibetan Plateau) during the last 340 years. Atmos. Environ. 176, 91–102.
Srivastava, S., Flora, S.J.S., 2020. Fluoride in drinking water and skeletal fluorosis: a review of the global impact. Current Environmental Health Reports 7 (2), 140–146.
Stein, A.F., Draxler, R.R., Rolph, G.D., Stunder, B.J., Cohen, M.D., Ngan, F., 2015. NOAA's HYSPLIT atmospheric transport and dispersion modeling system. Bull. Am. Meteorol. Soc. 96 (12), 2059–2077.
Tavener, S.J., Clark, J.H., 2006. Fluorine: friend or foe? A green chemist's perspective. Advances in Fluorine Science 2, 177–202.
Tian, L., Yao, T., MacClune, K., White, J.W.C., Schilla, A., Vaughn, B., Vachon, R., Ichiyanagi, K., 2007. Stable isotopic variations in west China: a consideration of moisture sources. J. Geophys. Res. Atmos. 112 (D10).
Torres-Sánchez, R., Sánchez-Rodas, D., de la Campa, A.S., Kandler, K., Schneiders, K., de La Rosa, J.D., 2019. Geochemistry and source contribution of fugitive phosphogypsum particles in Huelva,(SW Spain). Atmos. Res. 230, 104650.
Wang, C., Tian, L., Shao, L., Li, Y., 2019. Glaciochemical records for the past century from the Qiangtang Glacier No. 1 ice core on the central Tibetan Plateau: likely proxies for climate and atmospheric circulations. Atmos. Environ. 197, 66–76.
Wei, T., Brahney, J., Dong, Z., Kang, S., Zong, C., Guo, J., Qin, X., 2021. Hf–Nd–Sr isotopic composition of the Tibetan plateau dust as a fingerprint for regional to hemispherical transport. Environ. Sci. Technol. 55 (14), 10121–10132.
Weinstein, L.H., Davison, A., 2004. Fluorides in the Environment: Effects on Plants and Animals. Cabi, 2004.
Weinstein, L.H., 1977. Fluoride and plant life. J. Occup. Med. 19 (1), 49–78.
Xie, Z.M., Wu, W.H., Xu, J.M., 2003. Study on fluoride emission from soils at high temperature related to brick-making process. Chemosphere 50 (6), 763–769.
Xu, J., Kaspari, S., Hou, S., Kang, S., Qin, D., Ren, J., Mayewski, P., 2009. Records of volcanic events since AD 1800 in the East Rongbuk ice core from Mt. Qomolangma. Chin. Sci. Bull. 54 (8), 1411–1416.
Xu, X., Zhao, T., Lu, C., Guo, Y., Chen, B., Liu, R., Li, Y., Shi, X., 2014. An important mechanism sustaining the atmospheric "water tower" over the Tibetan Plateau. Atmos. Chem. Phys. 14 (20), 11287–11295.
Yang, Y., Zhang, R., Zhang, F., Li, Y., 2022. Spatial–temporal variation and health risk assessment of fluoride in surface water in the Tibetan plateau. Exposure and Health 1–17.
Yao, T., Masson-Delmotte, V., Gao, J., Yu, W., Yang, X., Risi, C., Sturm, C., Werner, M., Zhao, H., He, Y., Ren, W., Tian, L., Shi, C., Hou, S., 2013. A review of climatic controls on δ18O in precipitation over the Tibetan Plateau: observations and simulations. Rev. Geophys. 51 (4), 525–548.
Yao, T., Thompson, L., Yang, W., Yu, W., Gao, Y., Guo, X., Yang, X., Duan, K., Zhao, H., Xu, B., Pu, J., Lu, A., Xiang, Y., Kattel, D., Joswiak, D., 2012. Different glacier status

with atmospheric circulations in Tibetan Plateau and surroundings. Nat. Clim. Change 2 (9), 663–667.
Zhang, N., He, Y., Cao, J., Ho, K., Shen, Z., 2012. Long-term trends in chemical composition of precipitation at Lijiang, southeast Tibetan Plateau, southwestern China. Atmos. Res. 106, 50–60.
Zhang, W., Hou, S., Liu, Y., Wu, S., An, W., Pang, H., Wang, C., 2017. A high-resolution atmospheric dust record for 1810–2004 AD derived from an ice core in eastern Tien Shan, central Asia. J. Geophys. Res. Atmos. 122 (14), 7505–7518.
Zhao, C., Yang, Y., Fan, H., Huang, J., Fu, Y., Zhang, X., Kang, S., Cong, Z., Letu, H., Menenti, M., 2020. Aerosol characteristics and impacts on weather and climate over the Tibetan Plateau. Natl. Sci. Rev. 7 (3), 492–495.
Zhao, H., Yao, T., Xu, B., Li, Z., Duan, K., 2008. Ammonium record over the last 96 years from the Muztagata glacier in central Asia. Chin. Sci. Bull. 53 (8), 1255–1261.
Zhao, H., Xu, B., Yao, T., Tian, L., Li, Z., 2011. Records of sulfate and nitrate in an ice core from Mount Muztagata, central Asia. J. Geophys. Res. Atmos. 116 (D13).
Zhao, Z., Cao, J., Shen, Z., Xu, B., Zhu, C., Chen, L.W.A., Su, X., Liu, S., Han, Y., Wang, G., Ho, K., 2013. Aerosol particles at a high-altitude site on the Southeast Tibetan Plateau, China: implications for pollution transport from South Asia. J. Geophys. Res. Atmos. 118 (19), 11–360.
Zheng, W., Yao, T., Joswiak, D.R., Xu, B., Wang, N., Zhao, H., 2010. Major ions composition records from a shallow ice core on Mt. Tanggula in the central Qinghai-Tibetan Plateau. Atmos. Res. 97 (1–2), 70–79.
Zou, X., Hou, S., Wu, S., Zhang, W., Liu, K., Yu, J., Pang, H., 2020a. An assessment of natural and anthropogenic trace elements in the atmospheric deposition during 1776–2004 AD using the Miaoergou ice core, eastern Tien Shan, China. Atmos. Environ. 221, 117112.
Zou, X., Hou, S., Wu, S., Pang, H., Liu, K., Zhang, W., Yu, H., Song, J., Huang, R., Liu, Y., 2022. Ice-core based assessment of nitrogen deposition in the central Tibetan Plateau over the last millennium. Sci. Total Environ. 814, 152692.
Zou, X., Hou, S., Zhang, W., Liu, K., Yu, J., Pang, H., Liu, Y., 2020b. An increase of ammonia emissions from terrestrial ecosystems on the Tibetan Plateau since 1980 deduced from ice core record. Environ. Pollut. 262, 114314.